Investigations of CO_2-water wettability of coal: NMR relaxation method

Xiaoxiao Sun[a,b], Yanbin Yao[a,b*], Dameng Liu[a,b], Yingfang Zhou[c]

[a] School of Energy Resource, China University of Geosciences (Beijing), Beijing 100083, PR China

[b] Coal Reservoir Laboratory of National Engineering Research Center of CBM Development & Utilization, University of Geosciences, Beijing 100083, PR China

[c] School of Engineering, University of Aberdeen, Aberdeen, AB243UE, United Kingdom

Abstract

Carbon geo-sequestration (CGS) and recovery enhancement with carbon dioxide injection (CO_2-ECBM) have brought increasing focus on the CO_2 and water wettability of coal. The CO_2 and water contact angles measured using existing conventional methods, such as the pendent drop tilting plate technique and the captive-bubble technique, show low reproducibility due to coal heterogeneity and operational complexity. In this study, a novel NMR-based approach was developed to evaluate the CO_2 and water wettability of coal. The experimental results of nine bituminous and anthracite coals show that water wettability can be linearly correlated with the changes of the T_2 spectra peak positions. Based on the measured contact angle from the profile of the water adhering to the coal powder disc and the T_2 from the NMR of coal powder, we proposed a linear formulation to evaluate the contact angle using the change of T_{2g} of P3. Using this method, we analyzed the CO_2-water wettability characteristics of coal. The results show that CO_2 reduces the water wettability of coal. Low temperature and/or high CO_2 pressure can enhance the CO_2 wettability of coal. The change of water-coal wetting behavior with injection of CO_2, is resulted by three factors: change of CO_2 adsorption capacity of coal, change of interfacial tension, and dissolution of CO_2 in water. This study makes it possible to evaluate changes in the water and CO_2 wettability of coal, which is essential for evaluating the fluid-interaction mechanisms during the process of carbon geo-sequestration and enhanced coalbed methane recovery with carbon dioxide injection.

Keywords: CO_2 sequestration; coalbed methane; coal; wettability; relative permeability

1. Introduction

Coal seams offer great potential for carbon geo-sequestration (CGS) with the accompanying benefit of recovery enhancement with carbon dioxide injection (CO_2-ECBM) (Ozdemir, 2009; Gentzis, 2000; Busch and Gensterblum, 2011). CO_2 sequestration into coalbeds is largely controlled by the interactions between the coal matrix and CO_2 and other reservoir fluids. In particular, the wettability of coal controls the pore scale fluid configuration and thus has a strong effect on capillary pressure, relative permeability and fluid invasion mechanisms (Chalbaud et al, 2006; Chaturvedi et al., 2009; Han et al., 2010; Iglauer et al., 2015; Zhou et al., 2016).

In the context of reservoir engineering, coalbed methane (CBM) reservoirs consist of cleats and matrix pores that are saturated with water: fluid flows in large cleats according to Darcy's law,

whereas the diffusion-driven transport of gas occurs in coal micropores. The performance of CO_2 for CGS or CO_2-ECBM may be different for hydrophobic (gas-wet) and hydrophilic (water-wet) reservoirs. For a hydrophobic reservoir, micropores are occupied by gas, which leads to the much faster transport of the injected gas into the coal matrix. In contrast, if pores are filled with water, the transport of the injected gas in a hydrophilic reservoir is very slow due to the difficulty of gas diffusion through the water (Siemons et al., 2006; Kaveh et al., 2012). Hence, it is essential to quantify the wettability of coal to improve our understanding of the mechanisms of gas/water flow in coal seams.

Several quantitative and qualitative methods were used to evaluate the wettability of rock, including the contact angle measurement (Johnson and Dettre, 1969), the Amott method (Amott, 1959), the USBM wettability index (Donaldson et al., 1969), spontaneous imbibition (Bobek et al., 1958), the flotation method (American Petroleum Institute, 1962), displacement capillary pressure (Benner et al., 1942) and others (Meng et al., 2017). Among these methods, the Amott, USBM wettability index and displacement capillary pressure methods measure wettability by operating displacement tests. However, it is extremely difficult to perform these tests in unconventional low-permeable samples, such as coal and gas shale (Xu and Dehghanpour, 2014; Iglauer, 2017), which thus limits their application to wettability measurements. The spontaneous imbibition rate/volume test allows us to indirectly indicate the wettability of coal and gas shale (Gao and Hu, 2016), but it fails to obtain any quantitative index for wettability characterization. Similarly, the flotation method, which is a fast and simplified operations measurement, is strongly influenced by coal particle size and the distribution of coal powder on the water, even though it is commonly used in the coal cleaning and flotation industry (Fuerstenau et al., 1987). Moreover, determining the immersion time in the flotation method is subjective and depends on personnel experience since there is no explicit standard of judgment on the immersion time.

The contact angle measurement is the most commonly used method for research of the wettability of coal (Wei et al., 1992; Orumwense, 1998; Anderson, 1986; Arnold and Aplan, 1989). However, the evaluated coal wettability may sometimes be inaccurate using the contact angle measurement because coal is an extremely heterogeneous material with significant variation in its physical and chemical properties, even on a polished coal sample surface. According to Keller (1987), the coal compositions of paraffinic hydrocarbon, aromatic carbon, and minerals are strongly hydrophobic, intermediate water-wet and strongly water-wet, respectively. Therefore, the heterogeneity in coal composition can result in high wettability heterogeneity with non-uniform spatial contact angle distribution in a coal sample (Wei et al., 1992; Siemons et al. 2006). To reduce the uncertainty during wettability measurements resulting from coal heterogeneity, coal powder discs, instead of a polished raw coal surface, are normally used to measure the contact angle (He and Laskowski, 1992; Zhou et al., 2016). However, the effect of disc porosity on the contact angle has still not effectively been solved (He and Laskowski, 1992). Moreover, it is difficult to prepare the sample and to compress coal discs with a polished plane, especially for anthracite coal with low clay mineral content. Thus, it is urgent to develop a quantitative methodology, with simple operation and high accuracy, to determine the water wettability of coal to perform successful CGS and CO_2-ECBM projects.

In the context of CGS and CO_2-ECBM, it is of great value to investigate variations in the water and CO_2 wettability of coal that are affected by the in situ reservoir temperature and pressure, as well as the gas adsorption and solution (Saghafi et al., 2014b; Kaveh et al., 2012; Sakurovs and Lavrencic, 2011; Siemons et al., 2006). In the literatures, contact angle measurement methods, including the pendent drop tilting plate technique (Arif et al., 2016) and the captive-bubble technique (Kaveh, et al., 2011; Ibrahim and Nasr-El-Din, 2016), have been used to obtain water/gas wettability in high-pressure CO_2-water conditions. According to the results of Siemons et al. (2006), Sakurovs and Lavrencic (2011) and Kaveh et al. (2012), the contact angles of CO_2 gas bubbles against coal surfaces in water cells decrease with increasing gas pressure, indicating that the coal became more CO_2-wet. Additionally, there is a linear relationship between the gas bubble contact angle and gas pressure (Sakurovs and Lavrencic, 2011). Arif et al. (2016) measured the advancing and receding water contact angles of different rank coals using the pendent drop technique. They found that the CO_2 wettability is independent of coal rank, and it increases with gas pressure and decreases with temperature. In these works, the contact angle of water-coal or gas-coal is measured from the profile of the water/gas bubble adhering to the surface. There are two major challenges in these measurements: the first is conducting the measurement in a high-pressure water/gas filled cell, and the other is that the measurement must be completed quickly. However, it is problematic to perform the measurement quickly, especially for the captive gas bubble technique, as it requires enough time for CO_2 to adsorb on the coal. Additionally, the fast measurement may induce uncertainty in the contact angle. Moreover, for the contact angle measurement by the captive gas bubble method, the dissolution of gas bubbles in water also introduces inaccuracy to the results (Saghafi et al., 2014a). In addition to the mentioned challenges, the measured contact angle also depends on the gas bubble size. More specifically, smaller bubbles have higher capacity to wet coal (Saghfi et al., 2014b). In general, conventional contact angle measurement methods are not capable of evaluating the wettability of real water-CO_2-coal systems in reservoirs.

The low field ^1H Nuclear Magnetic Resonance (NMR) technique has been successfully used to quantitatively evaluate the wettability of porous media, such as conventional hydrocarbon reservoirs (Bortolotii et al., 2009; Johannesen et al., 2007; Zhang et al., 2000; Connolly et al., 2017) and soil (Manalo and Kantzas, 2003). For example, a recent research by Connolly et al. (2017) demonstrated that the successful use of the NMR to quantify capillary trapping during dynamic sandstone core flooding experiments at reservoir conditions. However, this method has not been applied successfully to measure the water-gas wettability of coal. In this work, we applied the NMR method to quantitatively characterize the wettability of coal. In contrast to existing methods, the NMR technique is nondestructive, fast and makes real-time measurements, in addition to providing reliable results. We also evaluate the changes in water wettability of coal under different CO_2 pressures and temperatures, which makes it possible to disclose the in situ interactions of fluids (water and CO_2) with coal in reservoir conditions. This study is significant for the following in-depth investigation of the potential effects of CO_2 and water wettability of coal on CGS and CO_2-ECBM.

2. Samples and methods

2.1. Samples

Nine coal block samples were collected from the underground coal mines of the Tarim, Ordos and Qinshui basins, China. All samples were carefully packed and immediately transported to the laboratory for vitrinite reflectance, maceral analyses and proximate analyses.

Six of the selected samples were crushed to powders of 0.18-0.25 mm in size. After moisture-equilibrium pretreatment, these powdered samples were conducted for CO_2 isothermal adsorption at a constant temperature of 25 °C and under pressures of up to 4.9 MPa following the Chinese GB/T 19560-2004 procedure.

2.2. Contact angle measurement

Contact angle measurements were performed on the high-pressure compressed disc artificial surface made from the powdered coal. Since coal is an extremely heterogeneous medium consisting of different macerals and minerals that have different surface properties, the crushed powder samples can average the surface of coal with different organic and in-organic compositions. To form a much smoother surface for the contact angle measurement, we used a very small particle size (0.074 mm) to prepare the powder samples. Each powder sample was dried in a vacuum-oven at 80 °C for 6 h and compacted at 30 MPa to form the coal discs. The compacted coal discs were kept in a vacuum container for constant angle measurements.

Contact angle measurements were conducted using an automatic contact angle meter equipped with 3 mega-pixel cameras and an LED light source. A special syringe and needle were used to fix the volume of the droplet to 10 μL to exclude the impact of drop size on the contact angle measurement. The profile of the drop on the coal discs was photographed through a zooming lens, and then the contact angle of the drop was measured (Fig. 1). The representative contact angles for each sample are the mean values of the contact angles measured on 30 different spots on each disc.

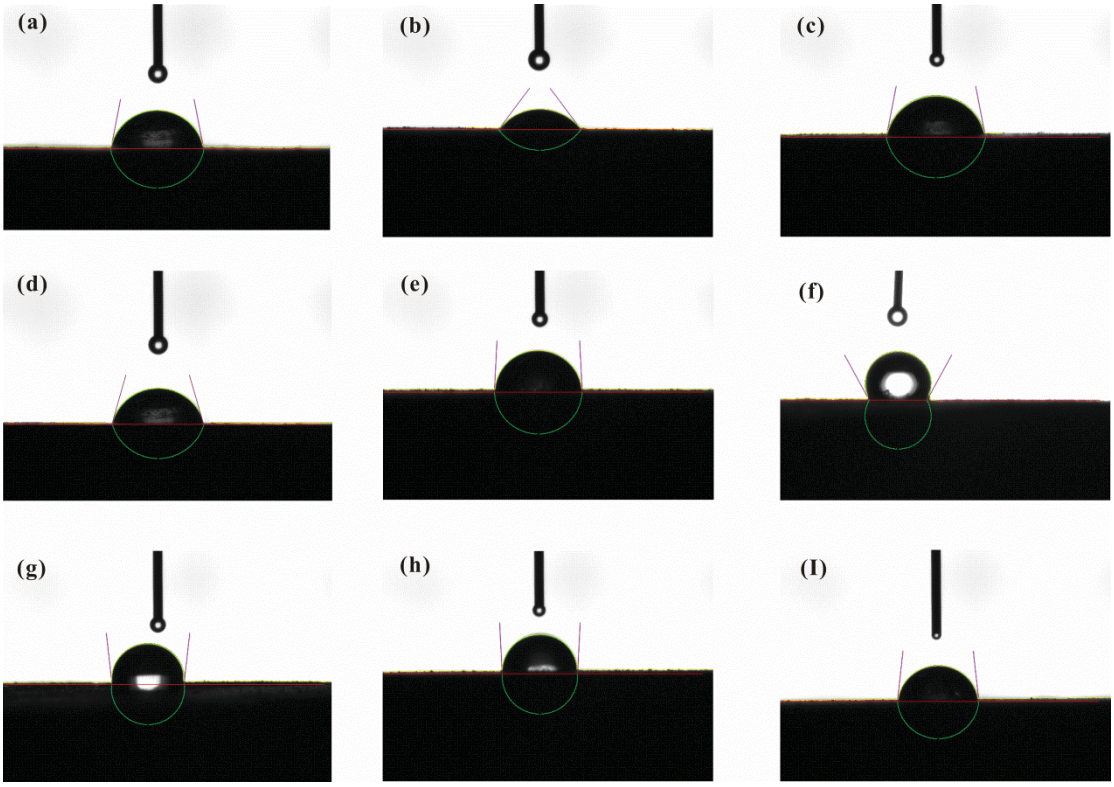

Fig. 1. Photographs of fluid-coal profiles for 9 samples (a-TA; b-FK; c-YX; d-SYQ; e-CYH; f-HY; g-GH; h-SJZ; i-WTP).

2.3. NMR measurements

The samples used for NMR measurements are powdered samples with coal particles of 0.18-0.25 mm. The powder samples were dried in a vacuum-oven at 80 °C for 6 h and then were put into a special made poly-Teflon sample cell for the NMR measurement. For the powdered samples in the sample cell, there are two types of pore voids: the inter-particle voids between coal particles, and intra-particle porosity within individual particles. It is well-accepted that the intra-particle porosity is much smaller than the inter-particle voids; thus, the intra-particle porosity can be neglected. Therefore, the inter-particle void porosity of packed coal powder can be calculated by:

$$\phi = 1 - \frac{m}{\rho V_c} \quad (1)$$

where □ is the inter-particle void porosity; V_c is the volume of the poly-Teflon sample cell; m is the powdered coal mass and ρ is the coal density. To keep all the samples in vials with the same void porosity, the same volume of coal powder was prepared by measuring the coal density ρ and coal powder weight. Then, we can obtain the same inter-particle void porosity by packing the coal powder with the same volume into the same vials. In this study, the inter-particle porosity of the sample, □, remains constant at 30%.

Four series of experiments, A-D, were completed (Table 1). For the sample preparation of the series A-D, coal powder and 1 mL of distilled water were put into the sample cell, and then the sample cell was wrapped with plastic sheeting to keep the surface water from evaporating and the coal powder from oxidizing. First, the wrapped sample cell was placed in the NMR magnetic coil

for experiment series-A. In this series, the T_2 spectra of nine samples were measured every hour to monitor the change of water in the coal. Second, experiment series-B was conducted on 6 coal powder samples to study the effect of CO_2 on the water wettability. In series-B, the relative changes of the T_2 spectra were measured at a constant 4-MPa CO_2 gas pressure and experimental temperature of 25 °C. Third, in series-C, the operation for samples SYQ and WTP was the same as experiment series-B except for the CO_2 pressures (2 and 6 MPa). Finally, experiment series-D was conducted for samples FK and GH with the same process as series-B except at different temperatures (35 and 45 °C). The purpose of conducting series-D is to investigate the effects of temperature on the water and CO_2 wettability of coal.

Table 1 Four experimental series and their experimental conditions

Experiment Series	Sample	Fluid	Pressure (MPa)	Temperature (°C)
A	TA,FK,YX, SYQ,CYH,HY GH,SJZ,WTP	Water	0.1	25
B	TA,FK, SYQ, GH,SJZ,WTP	CO_2	4	25
C	SYQ, WTP	CO_2	2 and 6	25
D	FK, GH	CO_2	4	35 and 45

In this study, the Carr–Purcell–Meiboom–Gill (CPMG) sequence was used to measure the T_2 distributions. The parameters of the NMR measurement are as follows: the echo spacing is 0.3 ms, the echo-train is 64, the wait time is 3 s and the echo number is 18000.

3. Results and discussion

3.1. Characterization of coal samples

The results of the vitrinite reflectance, maceral analyses and proximate analyses are listed in Table 2. The selected coals are high-volatile bituminous coal to anthracite coal, representing a broad range of coal ranks and litho-type compositions. The mean maximum vitrinite reflectance in oil (R_o, %) of the coal ranges from 0.8% to 3.13%. The coal macerals are mainly characterized by intermediate to high vitrinite corresponding to intermediate to low inertinite, plus minor proportions of liptinite.

The results of the CO_2 adsorption experiments are given in Table 3. The Langmuir volumes of the selected six coal samples range from 27.54 to 57.73 m^3/t (as-received-base), with the minimum value for the sample TA.

Table 2 Results of petrological composition analysis and coal proximate analysis of selected coals.

Sample ID	Basin	Coalmine	R_o[a]	Maceral and mineral (vol. %)				Proximate analysis (wt.%, dry)		
				V[b] (%)	I[b] (%)	L[b] (%)	MM[b] (%)	M_{ad}[c] (%)	A_{ad}[c] (%)	C_{daf}[c] (%)

TA	Ordos	Mutataian	0.8	66.5	21.4	7.9	4.2	1.74	9.75	72.94
FK	Tarim	Fukang	0.83	63.3	26.4	3.4	6.9	6.68	2.84	66.6
YX	Qinshui	Yuanxiang	0.9	70.1	21.7	3.5	4.7	1.19	11.38	71.72
SYQ	Ordos	Shangyuquan	0.95	65.3	23.2	5.4	6.1	4.13	23.5	73.12
CYH	Qinshui	Changyuhe	1.35	76.6	18.6	0.4	4.4	0.96	10.77	87.72
HY	Qinshui	Heyang	1.8	90.6	4.6	0	4.8	1.14	10.31	83.97
GH	Qinshui	Guohua	2.3	83.9	8.7	0	7.4	2.38	17.99	89.51
SJZ	Qinshui	Shenjiazhuang	2.77	80.6	10.4	0	9.0	1.03	14.64	85.06
WTP	Qinshui	Wangtaipu	3.13	89.2	2.2	0	8.6	1.42	18.08	97.47

[a]Mean maximum vitrinite reflectance in oil. [b]V, I, and L represent the volume percentages of vitrinite, inertinite and liptinite, respectively, in coal maceral composition. MM is the volume percentage of minerals in the air-dry base. [c]M_{ad} and A_{ad} represent the air-dry-base moisture content and ash yield, respectively. C_{daf} represents the dry-ash-free base fixed carbon content.

The measured contact angles for the nine samples vary from 53° to 118° (Table 3). Coal sample FK is the strongest water-wet, with a contact angle of 53°, whereas HY is the weakest water-wet, with a contact angle of 118°. The contact angle is related to coal rank and coal petrological composition. As shown in Fig. 2, the contact angles increase with coal rank at R_o values of 0.8%-1.8%, and then they decrease slightly with increasing coal rank at R_o values of >1.8%. The maximum of the contact angle is observed at coal rank from medium-volatile bituminous coal to low-volatile bituminous coal, which agrees well with the results reported by Horsley and Smith (1951). Moreover, contact angles show a positive correlation with vitrinite group contents (Fig. 2) because the vitrinite group is more hydrophobic than the inertinite group (Arnold and Aplan, 1989).

Table 3 The CO_2 isothermal adsorption analyses and contact angles of water on selected coal disc surfaces.

Sample ID	TA	FK	YX	SYQ	CYH	HY	GH	SJZ	WTP
Langmuir volume (m^3/t)	27.54	38.73	-	31.64	-	-	57.73	42.78	48.14
Langmuir pressure (MPa)	0.69	0.7	-	2.13	-	-	1.35	1.47	1.09
Contact angle(°)	79	53	79	74	87	118	96	93	84

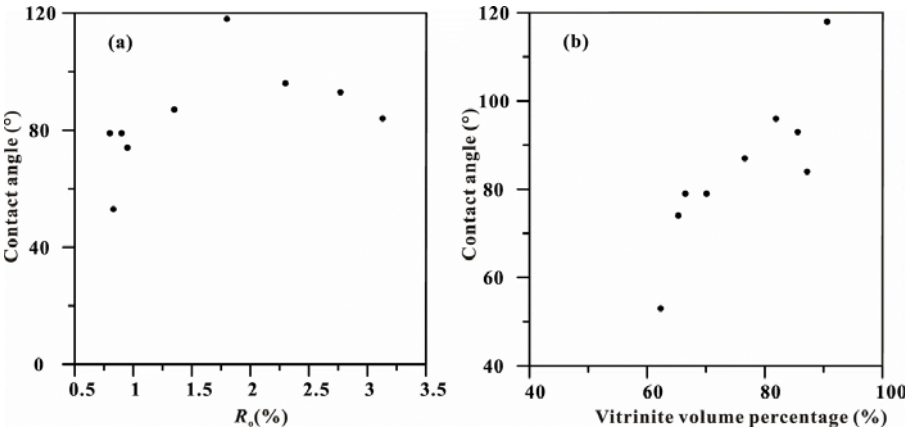

Fig. 2. The relationship between contact angles and a-mean maximum vitrinite reflectance in oil (R_o); b-volume percentage of the vitrinite group.

3.2. Determination of contact angle by the NMR method

3.2.1 Changes of T_2 spectra after water addition

According to the basics of NMR measurements, the T_2 of water in a homogeneous internal field gradient can be described by Eq. (2) (Howard et al., 1993; Kenyon et al., 1988),

$$\frac{1}{T_2} = \frac{1}{T_{2B}} + \rho_2 \frac{S}{V} \quad (2)$$

where B is bulk relaxation; ρ_2 is the surface relaxivity and S/V is the surface-to-volume ratio (Lowden et al., 1988). Bulk fluid relaxation relaxes slowly and signal peaks appear at longer relaxation times, which is an intrinsic property of the fluid. Surface relaxation relaxes rapidly and is affected by the interactions of the fluid with the surface (Coates et al., 1999; Yao et al., 2010, 2014).

The measured T_2 spectra of the coal powder samples with the addition of water indicate that different phases of water exist in the coal powder. As shown in the black solid line spectra in Fig. 3, there are three distinct T_2 spectrum peaks: P1, P2 and P3. P1, which is located at approximately 0.1-10 ms, represents the water in adsorption pores (with diameters of less than 0.1 μm) of individual coal particles. P2, located at approximately 10-100 ms, results from the surface relaxation of water in the seepage pores (more than 0.1 μm in diameter) of the individual coal particles (Sun et al., 2016). P3 (approximately 100-1000 ms) represents water in the inter-particle void space, which is dominated mainly by bulk water relaxation. Compared with the P1 and P3 peaks, the P2 peak appears to be too small. This means that the porosity of the seepage pores is relatively low in coal with a particle size of 0.2-0.3 mm (in diameter). Moreover, P2 is not detected for samples WTP and TA, which may result from the fast fluid exchange between bulk water and the water in the seepage pores.

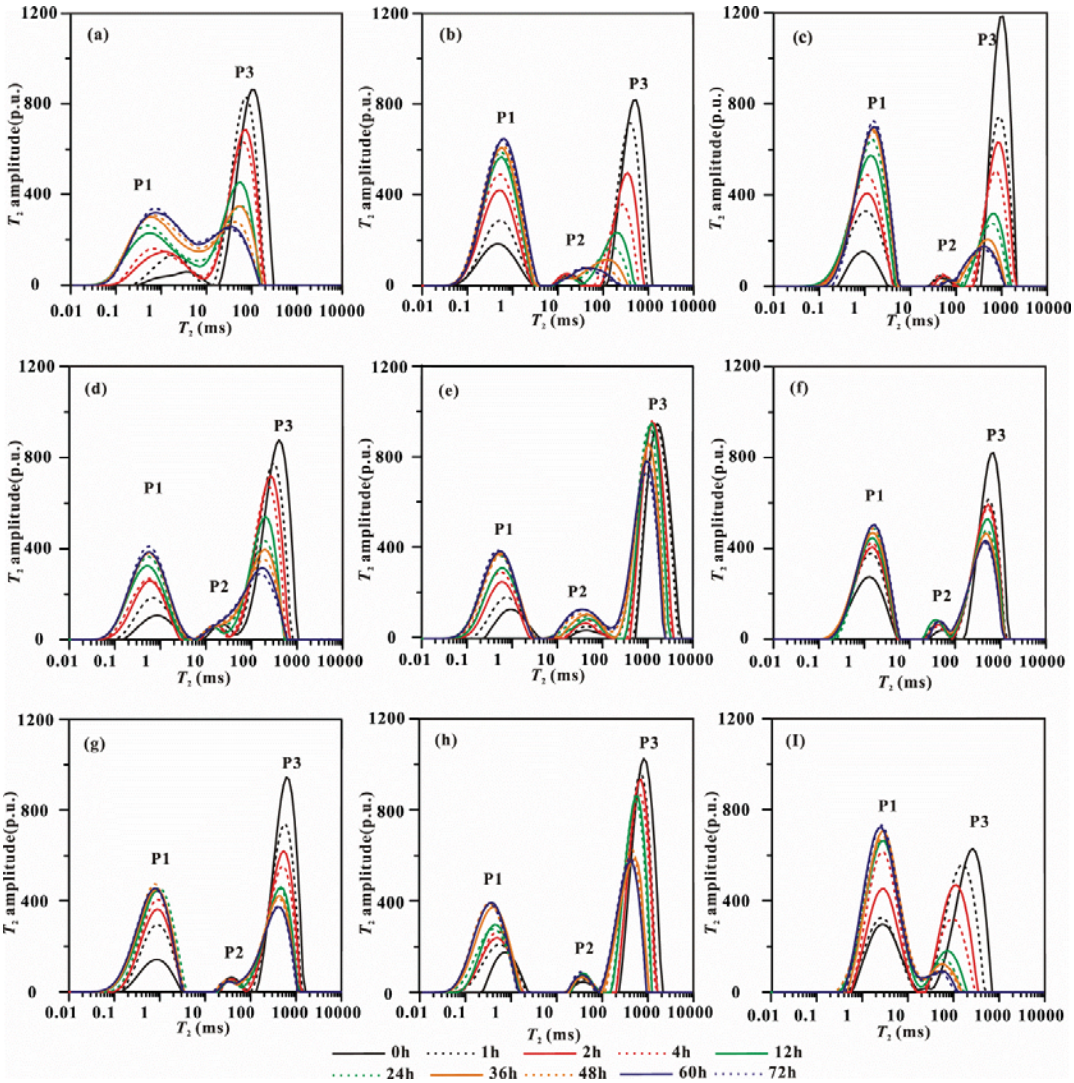

Fig. 3. T_2 spectra of coal samples after water addition (a-TA; b-FK; c-YX; d-SYQ; e-CYH; f-HY; g-GH; h-SJZ; i-WTP)

The different T_2 spectrum curves for the same coal sample in Fig. 3 show different water conditions within the coal sample, i.e., representing the movement of water in the coal powder with time. There is a notable trend of increasing P1 and decreasing P3 after the addition of water into the coal powder. Meanwhile, P3 shifts leftward (toward the fast relaxation part). This suggests that the bulk water in the inter-particle space moves into the intra-particle pores, leading to decreases in the area of P3 and increases in the area of P1. The changes of the P3 position indicate that the bulk water between individual particles spreads to more inter-particle surfaces. The movement of water leads to the T_2 relaxation being influenced more by the coal particle surfaces, resulting in the shift of P3.

To eliminate or reduce the negative effects of fluid interactions on the measurement results, the weighted average of T_2, T_{2g} (as defined in Eq. (3)), is used to quantify the change of peak position during a series of NMR measurements, and it is given as

$$T_{2g} = \exp[\sum \frac{\ln(T_{2i})A_i}{A_{total}}] \quad (3)$$

where T_{2g} is the weighted geometric average of the T_2 distribution, T_{2i} is the ith transverse relaxation time, A_{total} is the total signal amplitude of the T_2, and A_i is the signal amplitude of the ith T_2. A greater value of T_{2g} indicates that the fluid resides in larger pores or is more affected by the bulk phase; conversely, a smaller value reflects fluid residing in smaller pores. The change of T_{2g} indicates a shift of the T_2 spectra position, indicating the movement of fluid in pores (Guo and Kantzas, 2009). Thus, the T_{2g} of P3 is calculated to quantify the change in the peaks. Moreover, the normalized T_{2g} was used to measure the degree of peak changes for different coals.

Fig. 4 shows that the normalized T_{2g} of P3 decreases with water residence time for the nine coal samples. The reduction trends of T_{2g} are different from each other for these coal samples. For the same coal sample, the fastest decrease is noticed in the first 48 hours; then, the change decreases during 48-72 hours, which means the water in coal tends to approach an approximate equilibrium state after 48 hours. Thus, we assume that the water reaches an equilibrium state after 72 hours, when the change of the T_{2g} spectra between 60 to 72 hours can be neglected.

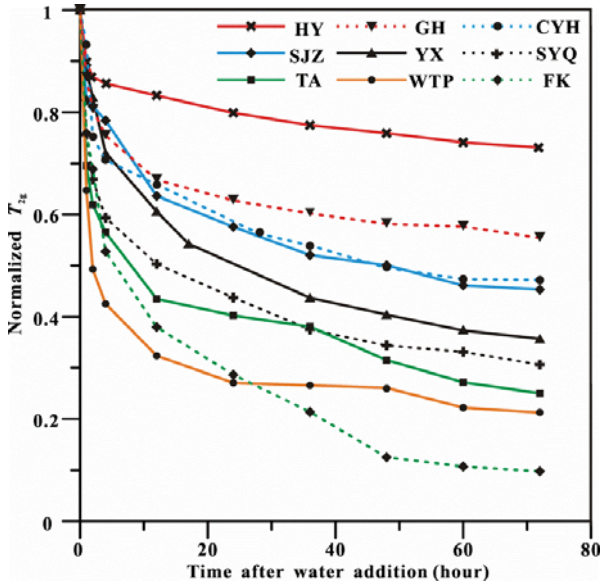

Fig. 4. The normalized T_{2g} of P3 decreases for different coals.

3.2.2. Determination of coal wettability by NMR

The ultimate normalized T_{2g} of P3 has a positive linear correlation against the measured contact angles for coal discs (Fig. 5). As shown in this figure, a smaller ultimate normalized T_{2g} of P3 value in the equilibrium state corresponds to a more water-wet coal sample. In contrast, a larger ultimate normalized T_{2g} of P3 value relates to a less water-wet coal. This is because for stronger water-wet coal, a large surface wettability force drives the water in the inter-particle space accesses into more coal particle surfaces. In this situation, the migration of water is represented by the leftward movement of T_2 distribution and a smaller T_{2g} value. We use the interfacial tension theory provided by Thomas Young (Young et al., 1805) to explain the mechanism of water migration. According to Young et al. (1805), the contact angle of a liquid drop on an ideal solid surface is defined by the mechanical equilibrium of the drop under the action of three interfacial tensions. The interactions between the three interfacial tensions are expressed by the Young-Laplace equation,

$$\delta_{sg} - \delta_{ls} = \delta_{lg}\cos\theta \quad (4)$$

where δ_{lg} is the gas-water interfacial tension; δ_{sg} is the gas-solid interfacial tension; δ_{ls} is the solid-water interfacial tension and θ is the contact angle of water on the solid surface. In Eq. (4), δ_{sg}-δ_{ls} is defined as surface wettability tension, which is the driving force of water migration on coal particle surfaces.

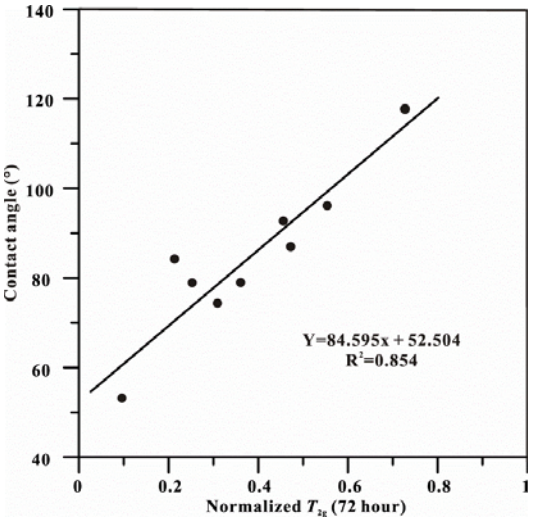

Fig. 5. The correlation between contact angles and ultimate normalized T_{2g} of P3 after the addition of water.

As mentioned above, for all samples, the inter-particle porosity and coal particle size are the same. Therefore, the different water spreading among coal powder results from different surface wettability tension for the coal samples. Moreover, the $\underline{\delta}_{lg}$ remains constant for different coal samples at the same conditions (temperature, pressure and media). Thus, there is a negative correlation between surface wettability tension and θ. For stronger water-wet coal with a small contact angle, a large surface wettability force drives the water to spread onto more coal particle surfaces. When the water in the inter-particle space spreads on more particles, the T_2 relaxation is influenced more by surface relaxation and leads to the T_2 value becoming smaller. Conversely, in the weaker water-wet coal powder, the water spreads to less coal particle surfaces, leading to slighter T_2 changes. Therefore, the changes of the T_{2g} of P3 show a positive correlation with surface wettability tension. Note that the gravity effect can be neglected for different coal powders because we used the same inter-particle porosity, coal particle size and experimental operations in this study.

As shown in Fig. 5, the contact angle of water on the coal surface, θ, could be correlated as a linear equation of T_{2g} of P3 at the end of the test (t=72 hours). The fitted linear correlation is given as below,

$$\theta = 84.6 \times T_{2g} + 52.5 \quad (5).$$

Eq. (5) is then applied as a general model to determine the contact angles of real coal samples based on the NMR measurements of the T_{2g} of P3.

3.2.3. Uncertainty analysis of the model

Assessing the reproducibility of the NMR experiments is important for evaluating the

credibility of the proposed model. In this study, we chose sample SJZ to repeat the NMR experiments at 25 °C. Two groups of reproducibility experiments were conducted for coal sample SJZ (Fig. 6a and 6b). Figure 6c compares the results from the two reproducibility experiments with those from experiment series-A. As shown in Fig. 6c, the T_{2g} values of P3, at the equilibrium state of water (72 hours), are almost the same for the three groups of experiments. The absolute deviation between the three sets of data at 72 hours after water dripping is within 1% for sample SJZ, which is acceptable in terms of deviation; thus, the model of wettability determination by NMR experiments is repeatable for all other samples.

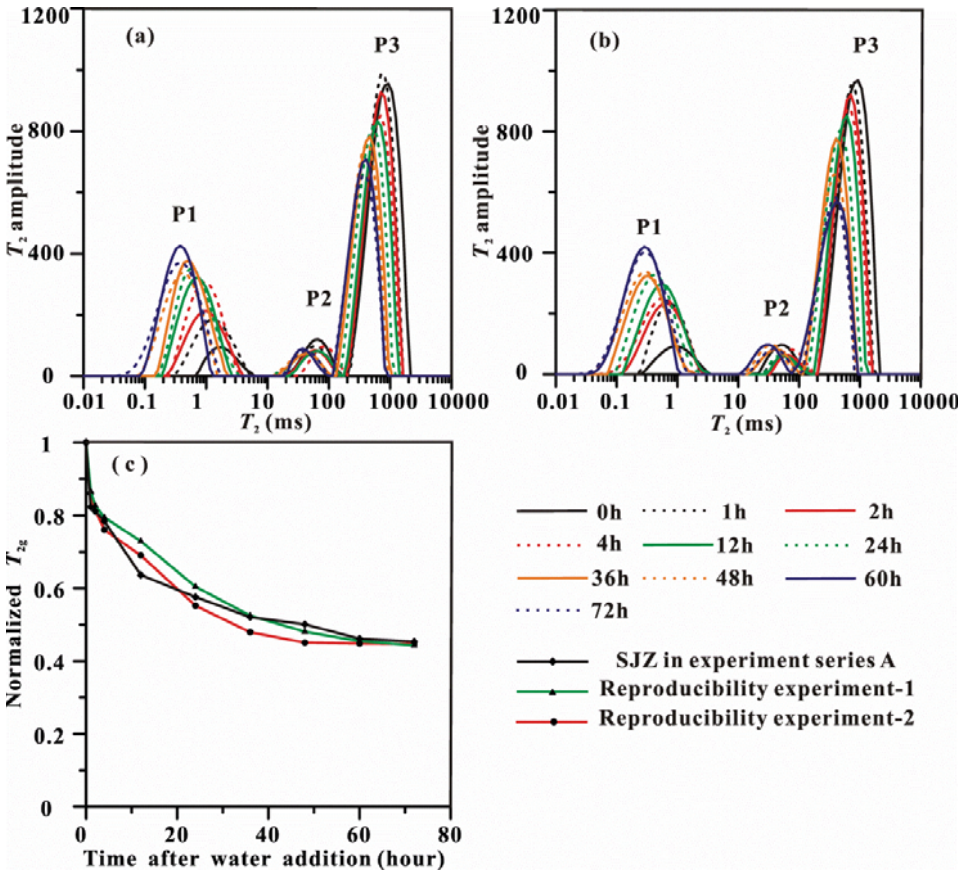

Fig. 6. a,b-Reproducibility experiments for the SJZ wettability measurement; c-The normalized T_{2g} of P3 peak decreases in the three groups of experiments.

However, there are two key uncertainties in the NMR wettability measurements. The first is related to the change in the coal mineral content during grinding and sieving. Jayaweera et al. (1989) concluded that ash content varied among different particle sizes, i.e., the ash content increased with decreasing mean particle diameter results from sieving method. In this study, we crushed and sieved using different size mesh sieves to get different size coal powders, and the remaining material on the topside sieve was crushed and sieved again. This procedure was continued until the whole portion eventually passed through the sieves. During the process of sieving, the minerals went through the sieves to smaller-sized coal powder. Thus, the mineral contents in the specific coal powder are slightly less than those of the raw coal samples. Another uncertainty is the coal oxidation during the 72-hour experiment. Although it is unavoidable, we attempted to keep the coal powder sample from oxidizing by accelerating the grinding operation

and then keeping the coal powder in a vacuum.

3.3 Effects of CO_2 injection on the change of water wettability of coal

After CO_2 injection into the coal reservoir, the reservoir properties (e.g., pore size distribution, permeability and wettability) will change due to a series of physical and chemical reactions between coal, water and CO_2 (Zhang et al., 2016; Iglauer, 2017). Thus, the laboratory analysis of water and the CO_2 wettability of coal can provide a better understanding of the simulation of underground CO_2 injection in the in situ reservoir.

In experiment series-B, six representative samples were selected from the nine coal samples in experiment series-A. The coal powders were kept in 4 MPa CO_2 after the addition of water, and then the T_2 spectra were measured to research the water wettability after the CO_2 treatment. Figure 7 shows the changes of the T_2 spectra after the water addition in CO_2 for the samples. Like the peak changes in experiment series-A, P1 increases and P3 decreases for all samples. Moreover, the P3 peak moves to the smaller T_2 with time. Comparing the normalized T_{2g} of P3 in experiment series-A and series-B for six samples shows that the normalized T_{2g} of P3 increases with the injection of CO_2 (Fig. 8). As discussed in the previous section, the increase of T_{2g} indicates that the spread of water on coal particle surfaces becomes weak for all samples in CO_2.

Experiment series-C and series-D were carried out to investigate the effect of pressure and temperature on the wettability changes of coal resulting from CO_2 injection. Figure 9 shows the T_2 spectra changes with time for samples SYQ and WTP under 2 MPa, 4 MPa and 6 MPa CO_2. Figure 10 shows the changes of normalized T_{2g} of P3 with time after the addition of CO_2 at different pressures. With pressure increasing from 2 MPa to 6 MPa, the normalized T_{2g} of P3 increases. The higher CO_2 pressure has a greater effect on the water spread on coal particle surfaces for both the bituminous and anthracite coals, which indicates that the high CO_2 pressure shows a positive effect on the decreases of water-wetting.

Figure 11 shows the change of T_2 spectra for samples FK and GH with time at 25 °C, 35 °C and 45 °C. With increasing temperature, the change ranges of the P3 area and position become larger. As shown in Fig. 12, after the addition of water and at different temperatures, the curves of normalized T_{2g} of P3 first decrease and finally tend to maintain a certain value. Moreover, the higher the temperature, the smaller the T_{2g} of P3, i.e., high temperature has a negative effect on the decrease of coal water wettability.

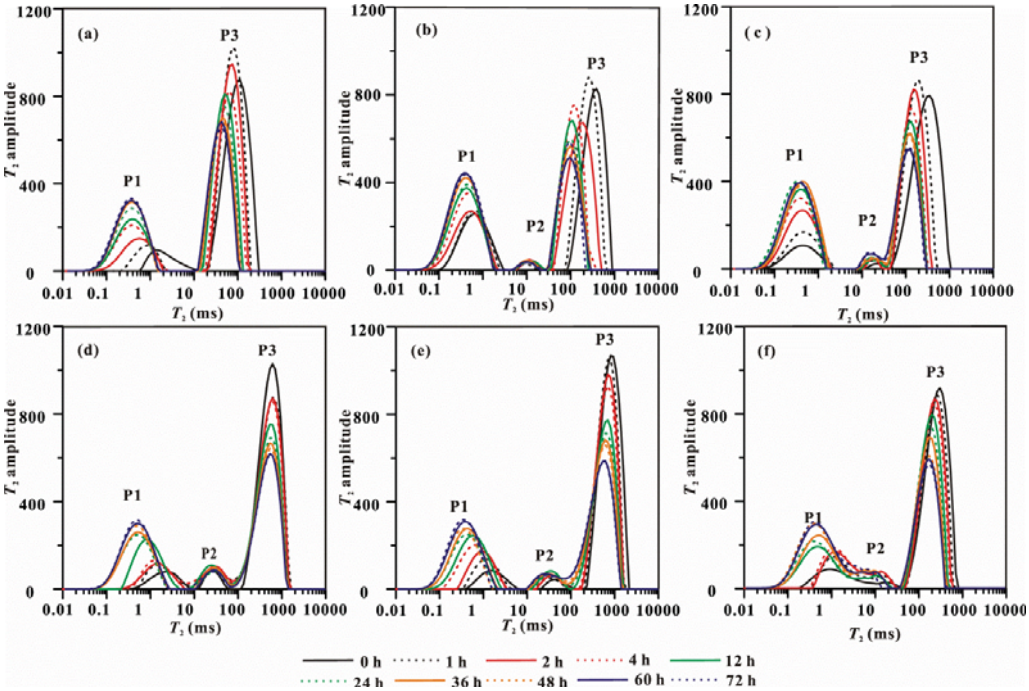

Fig. 7. T_2 spectra of coal samples after water addition in 4 MPa CO_2 (a-TA; b-FK; c-SYQ; d-GH; e-SJZ; f-WTP)

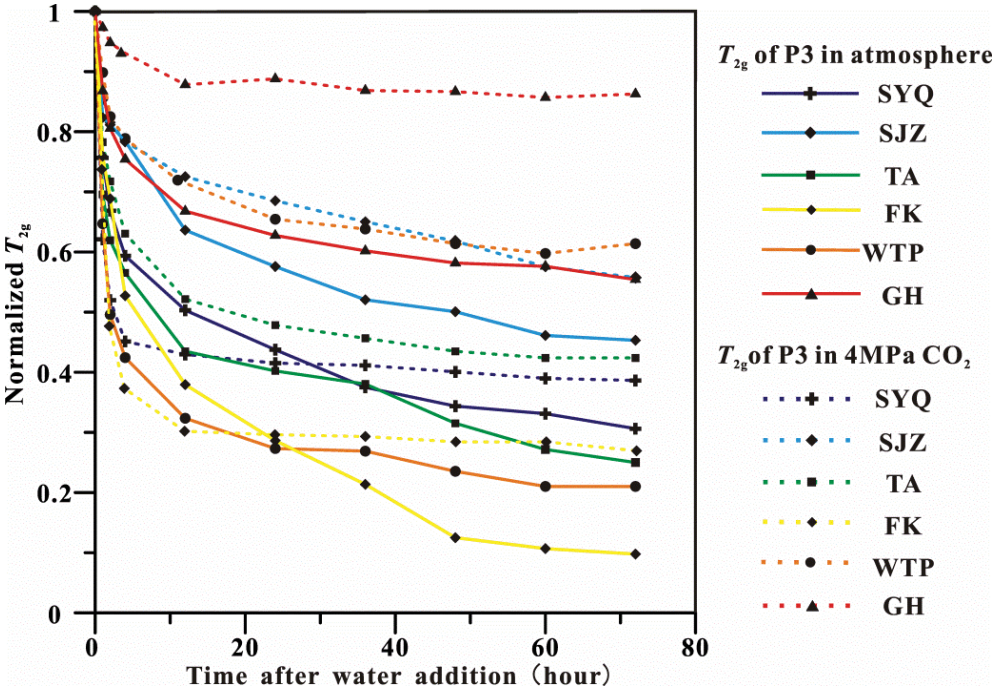

Fig. 8. The normalized T_{2g} of P3 decreases under atmospheric and CO_2 conditions

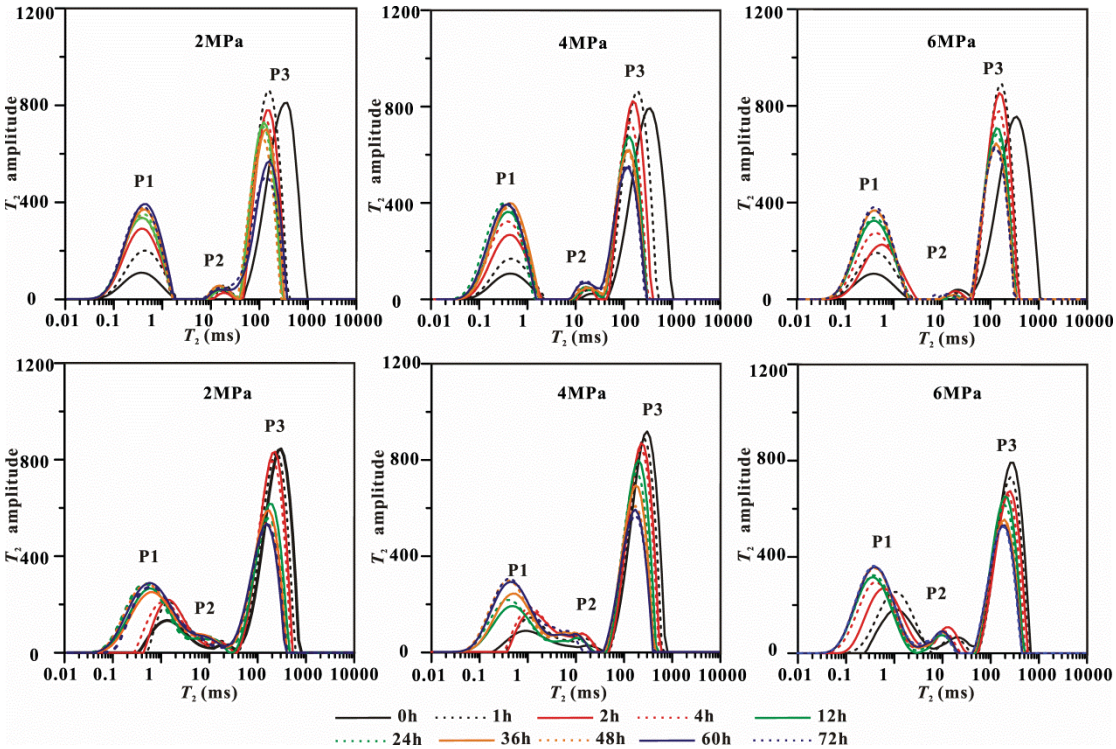

Fig. 9. T_2 spectra of coal samples at different CO_2 pressures after water addition (a,b,c-SYQ; d,e,f-WTP)

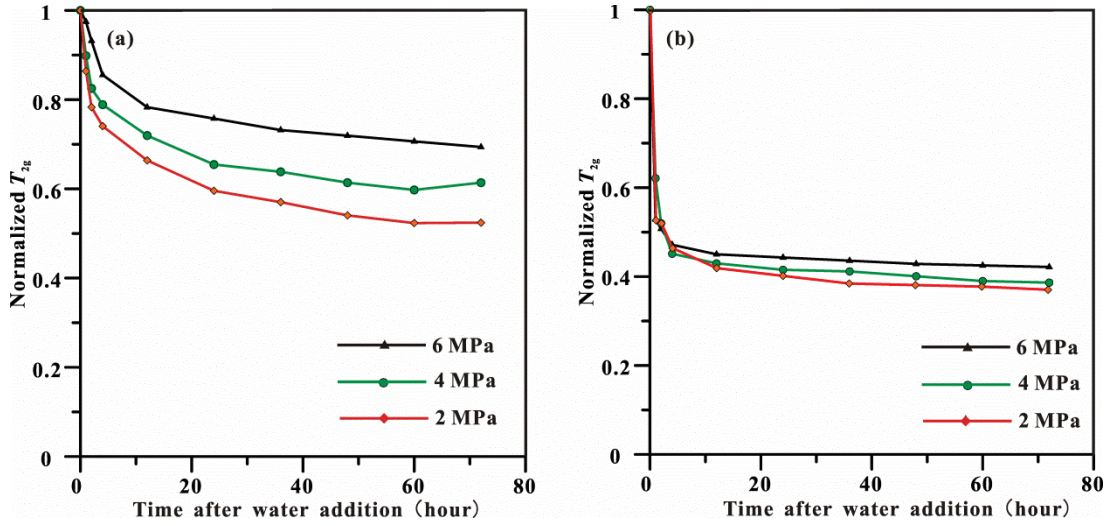

Fig. 10. The normalized T_{2g} of P3 decreases at different CO_2 pressures (a-WTP; b-SYQ)

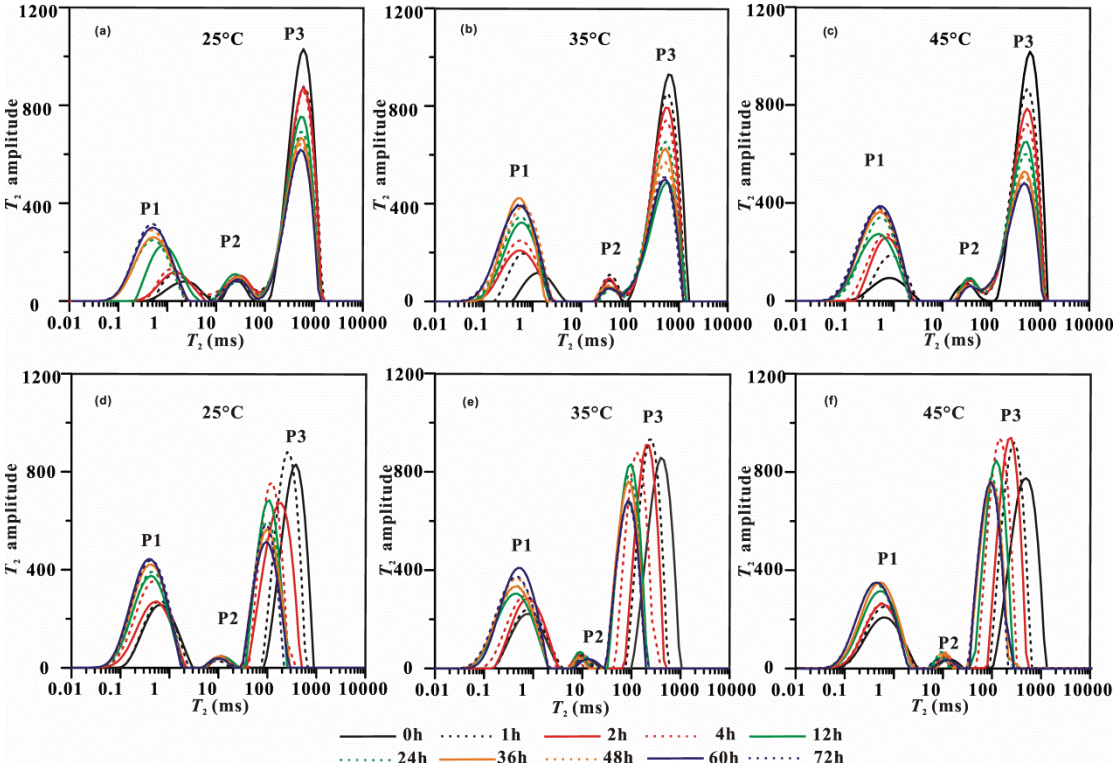

Fig. 11. T_2 spectra of coal samples after water addition at different temperatures (a, b, c-GH; d, e, f-FK)

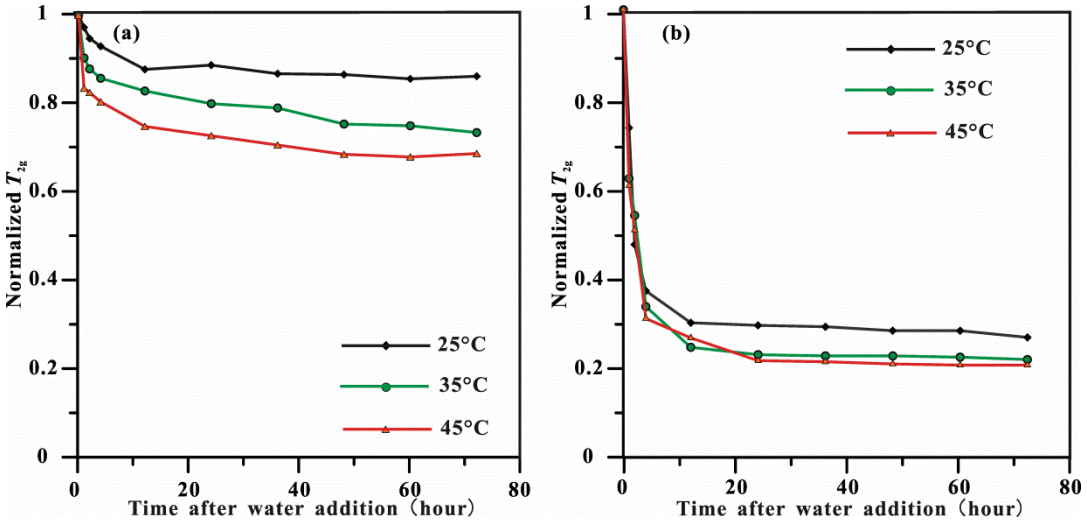

Fig. 12. The normalized T_{2g} of P3 decreases with CO_2 at different temperatures (a-GH; b-FK)

3.4 Discussion

3.4.1 Effect of coal properties on water and CO_2 wettability

The results of experiment series-B show that the T_{2g} of P3 increases with CO_2 injection and varies with different coal rank. Using Eq. (5) and the ultimate normalized T_{2g} of P3, we can obtain the contact angle of water in the 4-MPa CO_2 condition. As shown in Table 4, the contact angle of water increases with CO_2 injection, indicating that water wettability becomes weak for both anthracite and bituminous coals after being exposed to CO_2. However, the degree of change in wettability varies, and it is defined by the difference of the water contact angle between

experiment series-A and series-B ($\Delta\theta$) (Table 4).

Table 4 Water contact angle calculations using Eq. (5) in the series-A and series-B experiments

Sample ID	TA	FK	SYQ	GH	SJZ	WTP
water contact angle θ_1(°) (experiment series-A)	73.7	60.8	78.4	99.4	90.8	70.3
water contact angle θ_2(°) (experiment series-B)	88.4	84.7	85.2	125.5	99.7	104.4
$\Delta\theta(\theta_2-\theta_1)$	14.7	23.9	6.8	26.1	8.9	34.1

The $\Delta\theta$ is correlated with the CO_2 adsorption capacity, vitrinite content, fixed carbon content, and vitrinite reflectance of coal (Fig. 13). There is a slight positive correlation between the increase of the water contact angle and the CO_2 adsorption volume (Fig. 13a). Sakurovs and Lavrencic (2011) and Kaveh et al. (2011) suggested that the water-coal wetting behavior was affected by the adsorption of CO_2 on the coal surface. Although there is no proof of a direct relationship between CO_2 wettability and CO_2 adsorption, it can be assumed that coal with a large volume CO_2 adsorption capacity has stronger CO_2 wettability. Since adsorption is the dominant storage mechanism in coal, and it typically accounts for 98% of the total gas stored, further investigation is required to establish the relationship between CO_2-wettability and CO_2-adsorption. Moreover, the adsorption of CO_2 into micropores in the coal matrix leads to a significant decrease in permeability, which may limit the Darcy flow of the CO_2. A recent research by Zhang et al. (2016) demonstrated that CO_2 injection can change coal microstructure and permeability. Thus, further investigation is required to affirm whether the coal matrix swelling due to CO_2 injection is another reason for the change of CO_2 wettability or not.

The contact angle changes also show a slight positive relationship with vitrinite volume and fixed carbon content (Fig. 13b and c). As mentioned above, the vitrinite group is hydrophobic. Moreover, Sakurovs and Lavrencic (2011) found that the fixed carbon content increased the hydrophobicity of coal. Thus, those weak water-wet contents of coal may become more CO_2-wet during CO_2 injection. The relationship between coal rank (vitrinite reflectance) and $\Delta\theta$ is relatively weak (Fig. 13d).

3.4.2 The effect of pressure on water and CO_2 wettability

Experiment series-C shows that higher CO_2 pressure has a greater effect on the decrease of water wettability for both bituminous and anthracite coals, i.e., the coals become more CO_2-wet. To compare the water wettability of coal at different pressures, we calculated the contact angles of water using Eq. (5). The results are presented in Fig. 14. With increasing pressure of 0.1-6 MPa, the contact angle of water increased from 70.3° to 111.2° for WTP and from 78.4° to 88.2° for SYQ, which indicates the increase of CO_2 wettability. The increase of CO_2 wettability and the decrease of water wettability with CO_2 pressure are consistent with the existing experimental data. Sakurovs and Lavrencic (2011) experimentally determined the CO_2-coal contact angle using the

captive bubble technique for low to medium rank coal (R_o ranged from 0.62 to 1.4) and found an increase in CO_2 wettability with pressure for all samples. Siemons et al. (2006) measured the CO_2 contact angle for anthracite coal and found that it became CO_2-wet (θ>90) at 0.26 MPa. However, Arif et al. (2016) determined that semi-anthracite became weakly CO_2-wet at approximately 7 MPa (θ>110). Kaveh et al. (2011) found that semi-anthracite become CO_2-wet at 5.7 MPa and that high-volatile bituminous coal become CO_2-wet at 8.7 MPa. In our research, anthracite coal WTP became CO_2-wet at pressures of less than 2 MPa; however, bituminous coal SYQ became CO_2-wet at pressures of >6 MPa. As shown in Fig. 14, the contact angle changes more for anthracite than it does for bituminous coal with increasing pressure from 0 to 6 MPa.

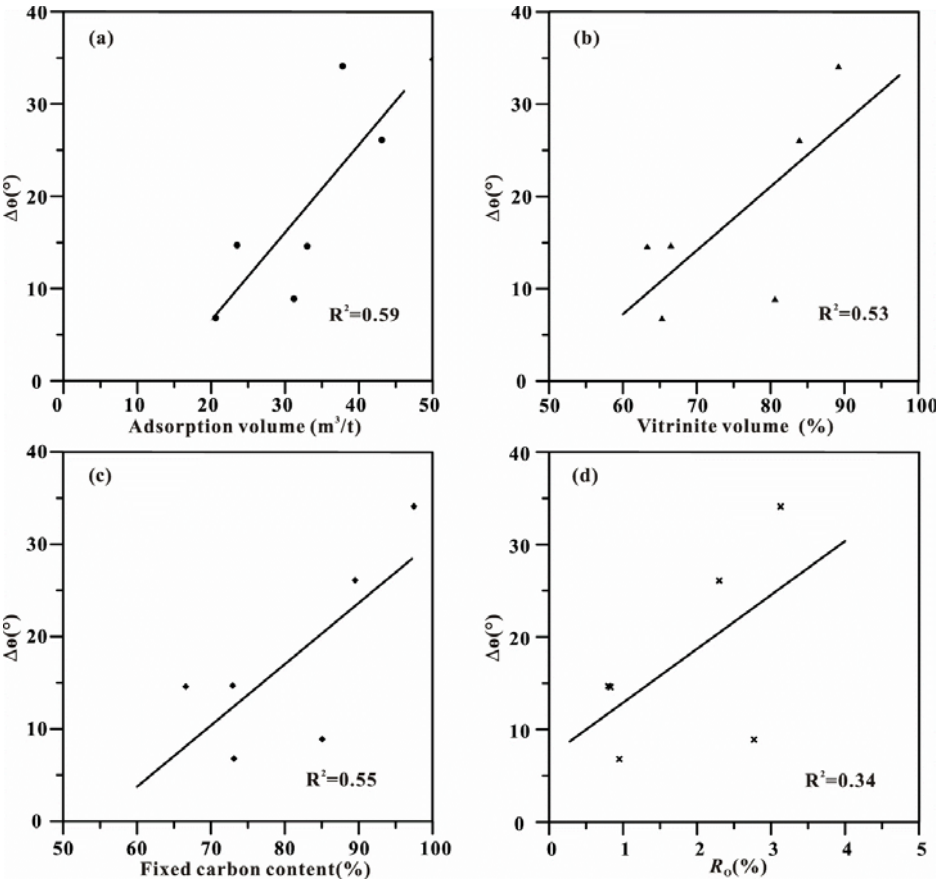

Fig. 13. The relationship between $\Delta\theta$ and a-CO_2 adsorption capacity; b-vitrinite volume content of coal; c-fixed carbon content of coal; d-mean maximum vitrinite reflectance in oil (R_o).

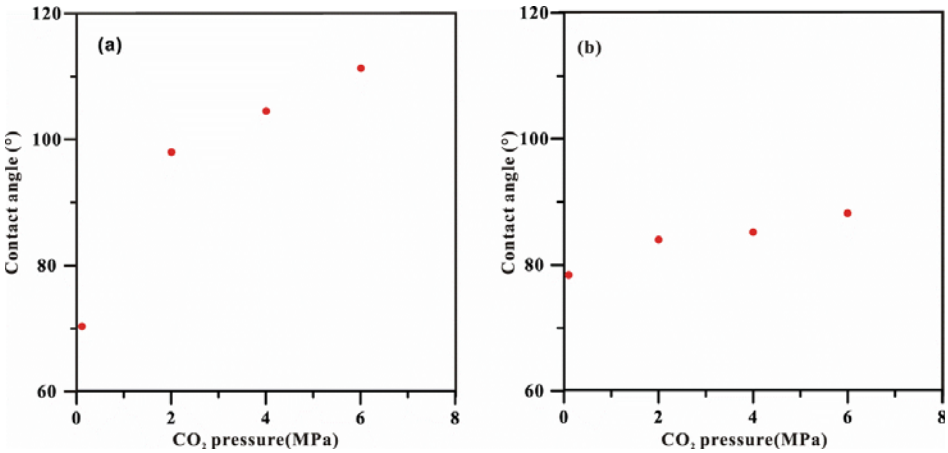

Fig. 14. The contact angle increases with increasing CO_2 pressure (a-WTP; b-SYQ)

According to previous studies (Kaveh et al., 2011; Sakurovs and Lavrencic, 2011; Siemons et al., 2006), three factors affect the water-coal wetting behavior with increasing CO_2 pressure, as shown in Fig. 15. The first one is the CO_2 adsorption capacity of coal. As discussed above, coal with higher CO_2 adsorption capacity is more CO_2-wet. The increase of CO_2 pressure leads to the more CO_2-wet (Fig. 15a). Moreover, similar trends in the literature data on CO_2 adsorption (Busch et al., 2003) also explain why the increased rate of contact angle is evident for pressures of 0.1-2 MPa in this study. The second factor is the change of interfacial tension with CO_2 pressure (Fig. 15b). Arif et al. (2016) indicated that the δ_{sg} of coal-CO_2 decreases with increasing CO_2 pressure (Fig. 15b). According to Eq. (4), surface wettability tension decreases with increasing CO_2 pressure. The third factor is CO_2 solution in water. The dissolution of CO_2 in water can decrease the pH, leading to the reduction of the negative charge density at the solid/water interface and thus reducing the electrokinetic potential of the coal particles (Ibrahim and Nasr-El-Din, 2016). Consequently, the δ_{ls} of coal-water increases due to the negative contribution of the electrostatic component to surface energy, which causes the surface wettability tension to become less effective in CO_2, according to Eq. (4). With increasing CO_2 pressure, the CO_2 solubility increases, leading to high H^+ concentrations (Wiebe and Gaddy, 1940); thus, the coal becomes more hydrophobic (Ibrahim and Nasr-El-Din, 2016).

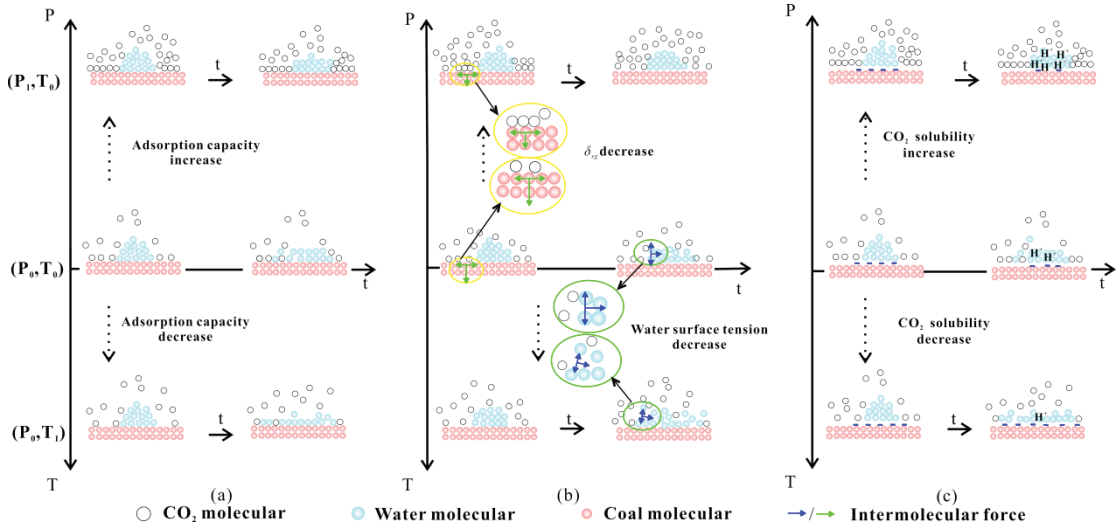

Fig. 15. The factors affecting the water-coal wetting behavior with pressure and temperature (a) CO_2 adsorption; (b) interfacial tension; (c) CO_2 dissolution

3.4.3 The effect of temperature on water and CO_2 wettability

As shown in Fig. 16, for both anthracite and bituminous coal at 4 MPa CO_2, the contact angle of water calculated by Eq. (5) decreases with increasing temperature. It can be concluded that high temperature decreases the effect of CO_2 on the water wettability of coal. For anthracite coal, there is a clear decrease from 125.5° to 110.7° with increasing temperature. However, for bituminous coal, the contact angle first decreases from 75.3° to 71.1° and then becomes almost constant. The impact of temperature on coal wettability after CO_2 treatment can also be explained by the three factors shown in Fig. 15. First, the increasing temperature reduces CO_2 wettability because high temperature reduces the CO_2 adsorption capacity of coal. The reduced CO_2 affinity makes coal more water-wet (Kaveh et al., 2011; Sakurovs and Lavrencic, 2011; Siemons et al., 2006; Ibrahim and Nasr-El-Din, 2016) (Fig. 15a). Second, increasing temperature induces the reduction of water surface tension (Gittens' research, 1969; Chiquet et al., 2007; Zhou et al., 2017) (Fig. 15b). The water contact angle decreases with temperature at 0.1 MPa without the solution and adsorption of CO_2 (Arif et al., 2016). Additionally, the decrease in contact angle with temperature has been reported for pure minerals such as mica or quartz (Chiquet et al., 2007). Finally, the water solubility of CO_2 decreases with temperature (Wiebe and Gaddy, 1940); thus, reduced H^+ concentrations can result in the increase of the water-wetting behavior of coal (Fig. 15c).

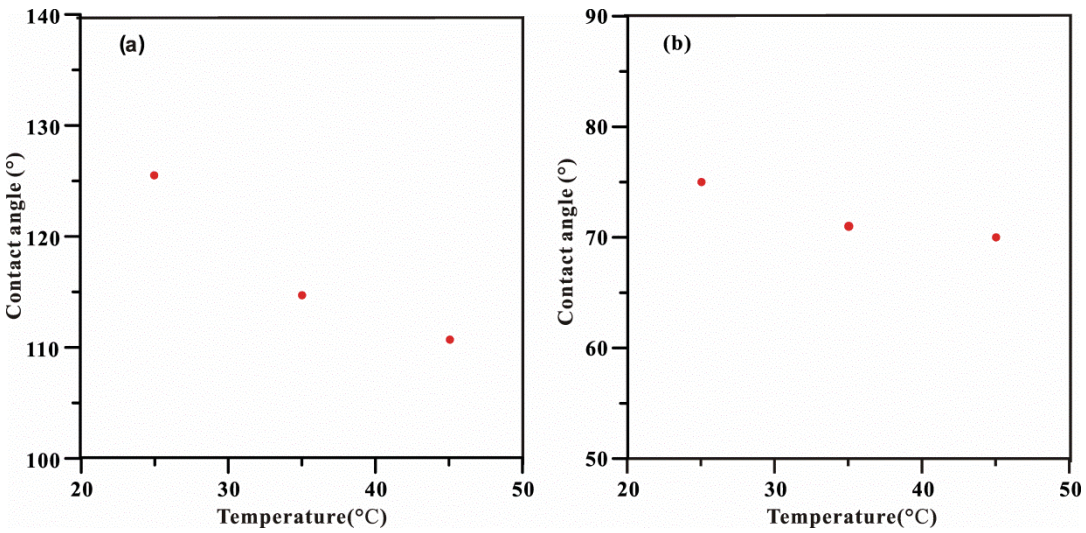

Fig. 16. The contact angles decrease with increasing temperature (a-GH; b-FK)

4. Implications

The NMR provides a novel technique to measure the water and CO_2 wettability of coal during CO_2 sequestration that can simulate in situ reservoir conditions. We determine the wettability of coal by fitting the T_{2g} of P3 and its contact angle against the coal surface. This method can also be used in other porous media, such as gas shale, although a different fitting formula must be established based on a series of measurements of NMR spectra and the contact angles of other

porous media.

The experimental data show that CO_2 storage in coal seams is strongly influenced by coal properties, gas pressure and reservoir temperature. The coal with high CO_2 adsorption capacity, high fixed carbon content and high vitrinite content shows more CO_2-wetting. Considering the fact that the sequestration capacity of coal is mainly dominated by CO_2 adsorption and the CO_2 wettability of coal, coal with high CO_2 adsorption capacity is more suitable for trapping CO_2. Therefore, CO_2 will occupy the micropores and water will occupy larger pores after CO_2 injection. Consequently, CO_2 will be distributed more uniformly in micropores and displace more methane and water. In addition, high CO_2 pressure and low reservoir temperature increase the CO_2-wettability of coal for both anthracite and bituminous coals. Consequently, high pressure and low temperature are two favorable factors for CGS and CO_2-ECBM.

5. Conclusion

In this study, water was dropped into coal powder and measured by NMR technology to determine the wettability of coal. The bulk water peaks of nine coal samples increase and shift to smaller T_2 values after the addition of water. The changes of the P3 position were quantitatively analyzed to determine the water wettability of coal. The wettability of coal from NMR results matches well with the contact angle measurements on coal discs. Although there are some uncertainties in the experiment, NMR provides a quantitative method to determine coal wettability.

NMR also provides a way to study water-CO_2 wettability with regard to coal properties, pressure and temperature. CO_2 injection can weaken the water wettability by replacing water from coal surface with adsorbed CO_2. Meanwhile, high CO_2 pressure increases the CO_2 wettability, and high temperature decreases the effect of CO_2 on the water wettability of coal. The change of water-coal wetting behavior with injection of CO_2, is resulted by three factors: change of CO_2 adsorption capacity of coal, change of interfacial tension, and dissolution of CO_2 in water. Analyzing wettability with NMR has the potential to target coal seams for CO_2 sequestration. Additionally, it can be used to determine the wettability of gas shale during CO_2 sequestration into gas shale reservoirs.

Acknowledgments

We acknowledge financial support from the National Natural Science Foundation of China (41472137), the Key Research and Development Projects of The Xinjiang Uygur Autonomous Region (2017B03019-01), and the National Major Research Program for Science and Technology of China (2016ZX05043-001), and the Royal Society Edinburgh and National Natural Science Foundation China (NSFC 41711530129).

Reference

American Petroleum Institute, 1962. API recommended practices for laboratory testing of surface active agents for well stimulation, American Petroleum Institute, Production Department.

Amott, E., 1959. Observations relating to the wettability of porous rock. Pet. Trans. AIME. 216, 156-162.

Anderson, W. G., 1986. Wettability literature survey-Part 2: Wettability measurement. J. Pet.

Technol., 38, 1246-1262.
Arif, M., Barifcani, A., Lebedev, M., Iglauer, S., 2016. CO_2-wettability of low to high rank coal seams: implications for carbon sequestration and enhanced methane recovery. Fuel 181, 680-689.
Arnold, B.J., Aplan, F.F., 1989. The hydrophobicity of coal macerals. Fuel 68, 651-658.
Benner, F.C., Dodd, C.G., Bartell, F.E., 1942. Evaluation of effective displacement pressures for petroleum oil-water silica systems. In: Drilling and Production Practice, New York, U.S.A.
Bobek, J.E., Mattax, C.C., Denekas, M.O., 1958. Reservoir rock wettability-its significance and evaluation. Pet. Trans. AIME. 213, 155-160.
Bortolotii, V., Macini, P., Falan, S., 2009. Combined spatially resolved and non-resolved ^{1}H NMR relaxation analysis to assess and monitor wettability reversal in carbonate rocks. In: International Petroleum Technology Conference, Doha, Qatar. SPE 13443.
Busch A., Gensterblum Y., Krooss B. M., 2003. Methane and CO_2 adsorption and desorption measurements on dry Argonne premium coals: pure components and mixtures. Int. J. Coal Geol.55, 205-224.
Busch, A., Gensterblum, Y., 2011. CBM and CO_2-ECBM related sorption processes in coal: A review. Int. J. Coal Geol. 87:49-71.
Chalbaud, C., Robin, M., Egermann, P., 2006. Interfacial tension data and correlations of brine-CO_2 systems under reservoir conditions. In: SPE Annual Technical Conference and Exhibition, San Antonio, Texas. SPE 102918.
Chaturvedi, T., Schembre, J.M. Kovscek A.R., 2009. Spontaneous imbibition and wettability characteristics of Powder River Basin coal. Int. J. Coal Geol.77, 34-42
Chiquet P., Broseta D., Thibeau S., 2007. Wettability alteration of caprock minerals by carbon dioxide. Geofluids 7, 112-122.
Coates, G. R., Xiao, L. Z., Prammer, M. G., 1999. NMR logging principles and applications. Gulf Publishing Company, Houston.
Connolly, P. R. J., Vogt, S. J., Iglauer, S., May, E. F., Johns, M. L., 2017. Capillary trapping quantification in sandstones using NMR relaxometry. Water Resour. Res. 53, 7913-7932.
Donaldson, E.C., Thomas, R.D., Lorenz, P.B., 1969. Wettability determination and its effect on recovery efficiency. Soc. Pet. Eng. J. 9, 13-20.
Fuerstenau, D.W., Williams, M.C., Narayanan K.S., Oiao, J.L., 1987. Assessing oxidation and the wettability of coal by a film flotation technique. In: 193rd ACS National meeting of the American Chemical Society, Denver, USA. Apr 5.
Gao, Z.Y., Hu, Q.H., 2016. Wettability of Mississippian Barnett Shale samples at different depths: investigations from directional spontaneous imbibitions. AAPG Bull. 100, 101–114.
Gentzis, T., 2000. Subsurface sequestration of carbon dioxide-an overview from an Alberta (Canada) perspective. Int. J. Coal Geol., 43, 287-305
Gittens, G. J., 1969. Variation of surface tension of water with temperature. J. Colloid Interface Sci. 30, 406-412
Guo, R., Kantzas, A., 2009. Assessing the water uptake of Alberta coal and the impact of CO_2 injection with low-field NMR. J. Can. Pet. Technol. 48: 40-46.

Han, F., Busch, A., Wageningen, N., Yang, J., Liu, Z., Krooss, B.M., 2010. Experimental study of gas and water transport processes in the inter-cleat (matrix) system of coal: Anthracite from Qinshui Basin, China. Int. J. Coal Geol.81, 128-138

He, Y.B., Laskowski, J.S., 1992. Contact angle measurements on discs compressed from fine coal. Coal Prep. 10, 19-36.

Horsley, R.M., Smith, H.G., 1951. Principles of coal flotation. Fuel 30, 54-63

Howard, J.J., Kenyon,W.E., Straley, C., 1993. Proton-magnetic resonance and pore-size variations in reservoir sandstones, SPE Form.Eval.3, 194-200.

Ibrahim, A. F., Nasr-El-Din, H. A., 2016. Effect of water salinity on coal wettability during CO_2 sequestration in coal seams. Energy Fuel 30, 7532-7542.

Iglauer, S. 2017. CO_2-water-rock wettability: variability, influencing factors and implications for CO_2 geo-storage. Acc. Chem. Res. 50, 1134-1142.

Iglauer, S., Pentland, C.H., Busch, A., 2015. "CO_2 wettability of storage and seal rock and implications for carbon geo-storage". Water Resour. Res. 51,729-774.

Jayaweera, S.A.A., Moss, J.H., Thwaites, M.W., 1989. The effect of particle size on the combustion of weardalecoal. Thermochim.Acta.152, 215-225.

Johannesen, E.B., Riskedal, H., Tipura, L., 2007. Wettability characterization by NMR T_2 measurements in Edwards limestone rock. In: International Symposium of the Society of Core Analysts, Calgary, Canada.

Johnson, R.E., Dettre, R.H., 1969. Wettability and contact angles. Surf. Colloid Sci. 2, 85-153.

Kaveh, N.S., Rudolph, E.S.J., Wolf, K.H.A.A., Ashrafizadeh, S.N., 2011. Wettability determination by contact angle measurements: hvbB coal-water system with injection of synthetic flue gas and CO_2. J. Colloid Interface Sci. 364, 237-247.

Kaveh, N.S., Wolf K.H., Ashrafizadeh S.N., Rudolph E.S.J., 2012. Effect of coal petrology and pressure on wetting properties of wet coal for CO_2 and flue gas storage. Int. J. Greenh. Gas Con. 11, 91-101.

Keller, D.V., 1987. The contact angle of water on coal. Colloids Surf. 22, 21-35.

Kenyon, W.E., Day, P.I., Straley, C., Willemsen, J.F. 1988. A three part study of NMR longitudinal relaxation properties of water saturated sandstones. SPE Form. Eval. 3, 622-636.

Lowden, B.D., Porter, M.J., Powrie, L.S., 1988. T_2 relaxation time versus mercury injection capillary pressure: implications for NMR logging and reservoir characterisation. In: European Petroleum Conference, Hague, Netherlands. SPE 50607.

Manalo, F., Kantzas, A., 2003. Soil wettability as determined from using low-field nuclear magnetic resonance. Environ. Sci. Technol. 37, 2701–2706.

Meng, Q., Liu, H., Huang, J.A., 2017. A critical review on fundamental mechanism of spontaneous imbibition and the impact of boundary condition, fluid viscosity and wettability. Adv. Geo-energ. Res. 1, 1-17.

Orumwense, F.O., 1998. Estimation of the wettability of coal from contact angles using coagulants and flocculants, Fuel 77, 1107-1111.

Ozdemir, E., 2009. Modeling of coal bed methane (CBM) production and CO_2 sequestration in coal seams. Int. J. Coal Geol.77, 145-152

Saghafi, A., Javanmard, H., Pinetown, K., 2014b. Study of coal gas wettability for CO_2 storage and CH_4 recovery. Geofluids 14, 310-325.

Saghafi, A., Pinetown, K., Javanmard H., 2014a. Gas wettability of coal and implications for gas desorption and drainage. In: 14th Coal Operators' Conference, University of Wollonong, Australia.

Sakurovs, R., Lavrencic, S., 2011. Contact angles in CO_2-water-coal systems at elevated pressures. Int. J. Coal Geol. 87, 26-32.

Siemons, N., Bruining, H., Castelijns, H., Wolf, K.H., 2006. Pressure dependence of the contact angle in a CO_2-H_2O-coal system. J. Colloid Interface Sci. 297, 755-761.

Sun, X., Yao, Y., Liu, D., Elsworth, D., Pan, Z., 2016. Interactions and exchange of CO_2 and H_2O in coals: an investigation by low-field NMR relaxation. Sci.Rep. 6, 19919.

Wei, D., Chander, S., Hogg, R., 1992. Distribution of wettability of coal. Int. J. Coal Prep. Util. 10, 37-45.

Wiebe, B.Y., Gaddy, V.L., 1940. The solubility of carbon dioxide in water at various temperatures from12 to 40° and at pressures to 500 atmospheres. J. Am. Chem. Soc. 62, 815-817.

Xu, M., Dehghanpour, H., 2014. Advances in understanding wettability of gas shales. Energy Fuels 28, 4362-4375.

Yao, Y.B., Liu, D.M., 2010. Petrophysical characterization of coals by low-field nuclear magnetic resonance (NMR). Fuel. 89, 1371-1380.

Yao, Y.B., Liu, D.M., Xie, S.B. 2014. Quantitative characterization of methane adsorption on coal using a low-field NMR relaxation method. Int. J. Coal Geol. 131, 32-40.

Young,T.,1805.An Essay on the Cohesion of Fluids. Philos. Trans. R. Soc. Lond. 95, 65-87.

Zhang, G.Q., Huang, C.C., Hirasaki, G.J., 2000. Interpretation of wettability in sandstones with NMR analysis. Petrophysics 41, 223-267.

Zhang,Y., Lebedev, M., Sarmadivaleh, M., Barifcani, A., Iglauer, S., 2016. Swelling-induced changes in coal microstructure due to supercritical CO_2 injection. Geophys. Res. Lett. 43, 9077-9083.

Zhou, G., Qiu, H., Zhang, Q., Xu, M., Wang, J., Wang, W., 2016. Experimental investigation of coal dust wettability based on surface contact angle. J. Chem. 9452303.

Zhou, Y., Hatzignatiou, D. G. and Helland, J. O., 2017. On the estimation of CO_2 capillary entry pressure: Implications on geological CO2 storage, Int. J. Greenh Gas Con, 63, 26-36.